Lifetime evaluation of ceramic materials

T. Fett, D. Munz
Kernforschungszentrum Karlsruhe,
Institut für Material- und Festkörperforschung IV,
and
Universität Karlsruhe,
Institut für Zuverlässigkeit und Schadenskunde im Maschinenbau

Abstract

The determination of subcritical crack growth data is necessary for lifetime predictions of real ceramic components. In this context the problem of measuring subcritical crack growth with natural cracks and macro-cracks is considered. It can be stated that the crack growth law for small natural cracks cannot be derived from measurements carried out with macro-cracks. For the determination of the v-K_I-relation with specimens containing natural flaws different methods are applied. Especially a lifetime method developed by the authors allows the determination of crack growth rates down to $1 \cdot 10^{-12}$m/s. Resulting v-K_I curves are reported for hot-pressed silicon nitride, Al_2O_3 and glass. Experimental results in cyclic fatigue are obtained for two alumina at room temperature and at 1100°C. From these tests a real cyclic fatigue effect can be concluded for the room temperature tests.

1. Introduction

Different failure modes are responsible for failure and finite lifetimes of ceramic materials. The most important of them are:

1.   spontaneous failure,
2.   subcritical crack growth under static load,
3.   cyclic fatigue,
4.   thermal fatigue,
5.   creep, creep crack growth, creep fracture.

Spontaneous failure occurs when the applied stress reaches the strength of the material, or in terms of fracture mechanics, when the stress intensity factor K of the most serious

crack in a component reaches or exceeds the fracture toughness K_{Ic}. Therefore, the knowledge of K_{Ic} is necessary to assess spontaneous failure behaviour.

Delayed failure at moderate temperatures can be caused either by subcritical crack growth, which is governed by the actual stress intensity factor K_I, or by crack propagation under cyclic load, which is governed by the stress intensity factor range ΔK and probably by the R-ratio defined as the quotient of minimum and maximum K-values.

Thermal fatigue at least combines the failure modes mentioned before. Additional effects such as oxidation may also have an influence.

In the *high-temperature* region, where pronounced creep occurs a structure can fail when excessive creep deformations become too large and the component stops functioning. In the creep range fracture can be caused by *creep crack growth* with the crack growth rates governed by the C*-integrals which are different for primary and secondary creep. *Creep fracture* describes the generation and accommodation of creep pores and their influence on fracture.

In this paper the items 2 and 3 will be treated in detail.

2. Failure by subcritical crack growth

2.1 General relations

The failure of ceramic components is often caused by subcritical crack propagation. In the range of linear-elastic fracture mechanics crack growth is governed only by the stress intensity factor K_I, which describes the stresses near a crack tip

$$\frac{da}{dt} = v(K_I) \tag{1}$$

K_I is defined by

$$K_I = \sigma\sqrt{a}\,Y \tag{2}$$

where σ denotes the stress and a the depth of a crack in a structure, and Y is the geometric correction factor dependent on the shape of the crack and the component. If the crack growth behaviour can be described by a power law

$$v = AK_I^n \tag{3}$$

one obtains a rather general *lifetime relation*

$$\int_0^{t_f}[\sigma(t)]^n dt = B\sigma_c^{n-2}\left[1 - \left(\frac{\sigma_f}{\sigma_c}\right)^{n-2}\right] \tag{4}$$

with

$$B = \frac{2}{A Y^2 (n-2) K_{Ic}^{n-2}} \qquad (5)$$

If $(\sigma_f/\sigma_c)^{n-2} < < 1$, a simplified form results

$$\int_0^{t_f} [\sigma(t)]^n dt = B\sigma_c^{n-2} \qquad (4a)$$

Equation (4) allows lifetime predictions based on pure subcritical crack growth for arbitrarily chosen time-dependent stresses.

2.2 Methods of determination of subcritical crack growth data

To allow correct lifetime predictions the relation (3) has to be known, especially for extremely low crack growth rates. Different methods of determining the v-K_I curves are available in the literature, e.g.,

- Double-Torsion (DT) method [1].
- Double-cantilever beam (DCB) technique [2].
- Controlled fracture test [3].
- Dynamic bending strength test [4].
- Lifetime measurements in static tests [5].
- Modified lifetime method [6].

The first three procedures are applied to macroscopic cracks on the order of several mm, but for lifetime predictions the crack growth behaviour of natural cracks of the order of 50μm is of interest.

It should be sufficiently known that the lifetimes of components with small natural cracks cannot be predicted satisfactorily from v-K_I curves obtained with specimens containing a large crack. This holds especially for materials with a strong R-curve effect where the crack growth of large cracks is significantly influenced by increasing toughness, whereas the effect on crack growth behaviour of small natural cracks is negligible. It was shown early by Adams et al [7] and recently by Chen et al [8] that the crack growth law for natural cracks is in contrast to macro-crack results. It was found that the exponents of the well-known power law are by a factor of 4 and more lower for natural cracks compared with the exponents for macro-cracks of several mm size. This behaviour is in agreement with own results reported in chapter 2.3 .

The dynamic bending test: From measurements of bending strengths at different stress rates $\dot\sigma$ one can evaluate n and B (or A). From eq.(4) one obtains

$$\sigma_f^{n+1} = B\sigma_c^{n-2}\dot{\sigma}(n+1)\left[1 - (\sigma_f/\sigma_c)^{n-2}\right] \qquad (6)$$

For very high loading rates ($\dot{\sigma} \rightarrow \infty$) it results $\sigma_f \rightarrow \sigma_c$. For low loading rates it follows asymptotically

$$\sigma_f^{n+1} = B\sigma_c^{n-2}\dot{\sigma}(n+1) \qquad (7)$$

Before the dynamic bending strength results can be evaluated with eq.(7) it must be ensured that the neglect leading from eq.(6) to eq.(7) is valid. Therefore, the evaluation of strength tests at only two stress rates is completely unsuitable. Figure 1 shows results obtained by Keller [9] on Y_2O_3-doped HPSN and results obtained by the authors for MgO-doped HPSN at high temperatures. For the Y_2O_3-doped material both limit cases can be identified easily. A least-squares fit including all strength values would give absurd n-values. Disadvantages of this procedure are:

- The type of v-K_I relation has to be known
- Inevitably, the bending strength is affected mainly by crack growth at a relatively high crack growth rate so that the crack growth parameters obtained are not necessarily characteristic of those crack growth rates which are of interest for lifetime predictions.

The lifetime methods: By combining eqs.(1) and (2) the lifetime formula for the static load test (σ = const.) results as

$$t_f = \frac{2}{\sigma^2 Y^2} \int_{K_{Ii}}^{K_{Ic}} \frac{1}{v(K_I)} K_I \, dK_I \qquad (8)$$

Very often, the assumption of a power law is made to evaluate the integral in eq.(8). By introducing eq.(3) in eq.(8) and taking into consideration $K_{Ii}^{n-2} \ll K_{Ic}^{n-2}$ the well-known *conventional lifetime relation*

$$t_f = B\sigma_c^{n-2}\sigma^{-n} \qquad (9)$$

results. As an application of this method static lifetime measurements from [10] are reported in fig.2 for hot-isostatically pressed Al_2O_3. They were carried out in 4-point bending tests in a concentrated salt solution at 70°C. From the slope and the position of the least-squares straight line the crack growth parameters were found to be

$$n = 20 \quad , \quad B = 0.3914 \text{ MPa}^2\text{h}$$

Apart from the invalidity of eq.(9) for short lifetimes due to the neglect during the derivation the weakness of this method is also the prescribed type of the special subcritical

crack growth law. The *modified lifetime procedure* is also based on eq.(8). Differentiation of eq.(8) with respect to the initial stress intensity factor K_{Ii} results in

$$v(K_{Ii}) = -\frac{2K_{Ic}^2}{Y^2\sigma_c^2 t_f} \frac{d(\ln K_{Ii}/K_{Ic})}{d(\ln t_f\sigma^2)} \tag{10}$$

In the derivation no special type of subcritical crack growth law is prescribed and there are no neglects relating to the upper limit of integration.

The needed change in K_{Ii} can be generated by introducing uniform small surface cracks, for instance by Knoop-indentation and variation of the bending stress applied or by use of a fixed stress and by making use of the scatter of the natural cracks. The first possibility is a very appropriate procedure if the initial size of the artificial cracks can be identified after the lifetime test.

For the second possibility the procedure of evaluation $v(K_I)$ is relatively simple. In a first series N samples are tested in dynamic bending tests at high stress rates in an inert environment to obtain the distribution of σ_c. The N values of strength are arranged in an increasing order. In a second series, also involving N specimens, the lifetimes t_f were measured. The results are also arranged in increasing order. The v-th value of lifetime $t_{f,v}$ is associated with the v-th value of inert bending strength $\sigma_{c,v}$. The latter is transformed into K_{Ii} using the relation

$$K_{Ii} = K_{Ic}\frac{\sigma}{\sigma_c} \tag{11}$$

The lifetime data represented in fig.2 were reevaluated and combined with inert strength data (for details see [10]). The resulting crack growth rates are given in fig.3. The results for the single stress levels are identical within the scatter band. In this case, the data can be well described by a simple power law similar to eq.(3). A least-squares fit yields an exponent n = 19 in accordance with the conventional procedure mentioned before. In fig.4 high temperature results (circles and triangles) obtained for hot-pressed silicon nitride are compared with the results of dynamic bending tests [11] (dashed-dotted lines). There is an excellent agreement between the two methods, both based on natural cracks.

2.3 Comparisons between small cracks and macroscopic cracks

The *static bending test with notched specimens* provides an appropriate way of determining the subcritical crack growth behaviour of macroscopic cracks. In a 3-point bending arrangement the specimen is statically loaded with load P (less than necessary for spontaneous failure) and the displacement δ is measured in the center of the sup-

porting roller span S by an LVDT. If the material shows subcritical crack propagation, the displacement δ does not remain constant but will increase with time. The amount of additional displacement after the elastic response ($\Delta\delta$) can be recorded whis a high resolution. Figure 5 shows a displacement vs. time curve for an Al_2O_3 -ceramic tested at 20°C in air. Immediately after load application a high displacement rate $\dot{\delta}$ appears which becomes reduced with increasing time, and only shortly before the specimen fails $\dot{\delta}$ arises again. The displacement increment $\Delta\delta$ is caused by a change of the compliance C, which is a direct consequence of a crack extension Δa. It holds

$$\Delta C = \Delta\delta \, / \, P \tag{12}$$

From the actual compliance C the crack depth a can be evaluated for any time. The only fracture-mechanical quantity necessary for the evaluation of this static *macroscopic crack growth test* is the geometric function Y for the crack-load-configuration. The function Y for S/W = 8 - based on numerical results of Gross and Srawley [12] - can be expressed by

$$Y = \frac{1}{(1 + 2a)(1 - a)^{3/2}} \, [\, 1.99 -$$

$$-\frac{a(1 - a)}{(1 + a)^2} (1.4925 + 0.685a - 2.8325a^2 + 2.085a^3 + 1.35a^4)] \tag{13}$$

for $0.1 \leq a < 1$.

The relation between the relative crack depth $a = a/W$ and the compliance C is simply given by

$$C = C_0 + \frac{9}{2} \, \frac{S^2}{W^2 EH} \int_0^a Y^2 a' \, da' \tag{14}$$

where

$$C_0 = \frac{S^2}{W^2 HE} \left[\frac{S}{4W} + \frac{(1 + v)W}{2S} \right]$$

is the compliance of the unnotched bending bar. E is the Young's modulus, v denotes the Poisson ratio, and H is the width of the specimen. A numerical evaluation of the integral in eq.(14) yields after curve fitting

$$C = C_0 + 1.99^2 \, \frac{9}{4} \, \frac{S^2}{W^2 EH} \, \frac{a^2}{(1 - a)^2 (1 + 3a)} \, [\, 1 - 0.8953a + 0.69655a^2 - 0.38523a^3]$$

$$\tag{15}$$

within $\pm0.2\%$ for $0 \leq a \leq 0.95$.

Knowledge of the crack depth, a, allows to compute the actual stress intensity factor with eq.(2). In fig.5 the time-dependent crack depth and the stress intensity factor are plotted in addition. A comparison of the K_I-values with the fracture toughness of 3.8 MPa$\sqrt{m}$ (obtained in a fast load-rate controlled 3-point bending test) illustrates a significant R-curve behaviour. Finally, the v-K_I curve results if the time derivative of the a(t)-curve is taken. In fig.6 this macro-crack v-K_I curve is plotted in addition to the v-K_I relation obtained from static lifetime measurements on specimens with natural crack population. It must be stated that only at the beginning of the macro-crack bending test the high crack rates - expected from the natural cracks - occur. After a small amount of crack extension the crack growth rate drops by several magnitudes. From this result it becomes evident that lifetime predictions for specimens with natural cracks cannot be based on "macro-crack results".

A second example may support this statement. From the results in figs.3 and 4 an unusually low crack growth exponent $n \simeq 20$ was concluded ([10]). The identical material was also investigated in DT-tests by Hermansson [13]. The resulting v-K_I curves showed very high n-values in the range of $150 \leq n \leq 410$ in complete contrast to the natural crack results. The mean-value curve reported in [13] is compared with the data of figs.3 and 4. and additionally plotted in fig.7 as solid line.

An obvious indication of the existence of a strong R-curve effect is the difference of the K_{Ic} value which was 4.0MPa$\sqrt{m}$ for the edge-notched bending specimen and 6.0-6.4 MPa$\sqrt{m}$ in the DT-test.

Both examples demonstrate the weakness of large crack tests and the enormous problems of transferability of the results obtained on small natural cracks.

3. Cyclic fatigue

Cyclic fatigue of ceramics with natural cracks can be caused by subcritical crack growth determined from static tests. In addition "real" fatigue damage may occur. This cyclic effect can be proved by comparing cyclic lifetimes from experiments with predictions from static tests as shown in the following chapter.

3.1 General relations

By introducing into eq.(4a) a periodical stress with a period T and a mean stress $\overline{\sigma}$

$$\sigma(t) = \overline{\sigma} + \sigma_a f(t) \quad , \quad f(t) = f(t + T) \tag{16}$$

into eq.(4a) and by assuming that only the positive stress parts σ^+ cause subcritical crack growth it results for the lifetime in the cyclic test

$$\frac{t_{fc}}{T} \int_0^T (\sigma^+)^n dt = B\sigma_c^{n-2} \tag{17}$$

Case R$\geq$0: If the stress ratio $R = \sigma_{min}/\sigma_{max}$ is positive, one obtains the lifetime in a cyclic test t_{fc} from the lifetime of a static test t_{fs} performed at stress σ_s:

$$t_{fc} = t_{fs}\left(\frac{\sigma_s}{\overline{\sigma}}\right)^n \frac{1}{g(\sigma_a/\overline{\sigma}, n)} \quad ,\text{with} \quad g = \frac{1}{T}\int_0^T \left[1 + \frac{\sigma_a}{\overline{\sigma}} f(t)\right]^n dt \tag{18}$$

Case R$<$0: In this case negative stresses occur which do not make contributions to the integral in eq.(17). As an additional problem, the mean stress may vanish. Therefore, in this case a different treatment is appropriate. If the stress is sinusoidal

$$\sigma(t) = \overline{\sigma} + \sigma_a \sin(\frac{2\pi}{T} t)$$

it results

$$t_{fc} = t_{fs}\left(\frac{\sigma_s}{\sigma_a}\right)^n \frac{1}{h(\overline{\sigma}/\sigma_a, n)} \tag{19}$$

where

$$h(\frac{\overline{\sigma}}{\sigma_a}, n) = \frac{1}{\pi}\int_{-a}^{\pi/2} [\overline{\sigma}/\sigma_a + \sin\varphi]^n d\varphi \quad \text{with} \quad a = \arcsin(\overline{\sigma}/\sigma_a) \tag{20}$$

If especially the cyclic lifetime is compared with static lifetimes measured with the upper stress t_{fs}^* it holds

$$t_{fc} = \frac{1}{h}(1 + \frac{\overline{\sigma}}{\sigma_a})^n t_{fs}^* \tag{21}$$

3.2 The alternating test (R = -1)

Cyclic fatigue includes as well subcritical crack growth as an effect of the cycles. The higher the R-ratio is the higher is the influence of subcritical crack extension, and the share of the additional cycles diminishes. For R = 1 only pure subcritical crack growth remains. From this point of view, the ratio R = -1 seems to be most promising in studying cyclic effects.

For this case, the function h can be expressed analytically by

$$h(0,n) = \frac{1}{2\sqrt{\pi}} \frac{\Gamma(\frac{n}{2} + \frac{1}{2})}{\Gamma(\frac{n}{2} + 1)} \tag{22}$$

3.3 Results

For each of the two cases mentioned before an example will be reported.

Case R > 0: Figure 8 shows results of 4-point-bending tests on Al_2O_3 containing 2.7% SiO_2 [15]. The tests are carried out at 1100°C with an elastically calculated mean stress $\overline{\sigma} = 60MPa$ and $R = 0.2$ at different frequencies.
A linear-elastic lifetime prediction was made based on results of static bending tests. Therefore, static lifetimes were measured at the same upper stress of 100MPa. The predicted lifetimes for cyclic tests - based on eq.(18) - are plotted in the left part of fig.8.

There are two reasons for the absence of a cyclic fatique effect of this material for the chosen test conditions

1. Within the scatter of the lifetimes there is no significant influence of the frequency obvious.

2. The predicted lifetimes are nearly identic with the measured ones.

The following general problem is important in most high-temperature tests: The formulae represented before were derived for pure linear-elastic fracture mechanics. At high temperatures, ceramics can exhibit a pronounced creep behaviour, which will affect static and cyclic lifetime tests in a different way. Whilst for the static tests the K_I-concept can fail and the crack extension may be governed by C^* -controlled creep crack growth, the cyclic tests with its fast stress changes will also exhibit K_I-controlled crack propagation. In such cases where different failure modes are responsible for failure a prediction of cyclic tests by static tests is not longer correct. In addition, the stress redistributions in the bending bar caused by creep will be different under both loading conditions.

Case R = -1: Figure 9 shows the result of lifetime measurements on Al_2O_3 at room temperature in cantilever beam tests performed under pure alternating load at a frequency of 50Hz for specimens with natural cracks as well as artificial Knoop cracks. From the results of static tests the corresponding cyclic lifetimes were calculated using eqs.(21) and (22). Whereas in the static bending tests only one side is under tensile loading, failure can occur at both sides in the alternating bending test, i.e. the effective surface of the specimens in cyclic tests is twice the surface in static tests. This has to be taken into

consideration for the failure prediction of the specimens with natural flaws. From these tests a real cyclic fatigue effect can be concluded for both types of cracks.

4. References

[1]   E.R. Fuller, "An evaluation of double-torsion testing - Analysis", Fracture Mechanics Applied to Brittle Materials ASTM STP 678,1979,3-18.

[2]   S.W. Freiman, D.R. Murville, P.W. Mast, "Crack propagation studies in brittle materials", J. Mater. Sci. 8 1527-1533(1973).

[3]   F.W. Kleinlein, "Langsame Rißausbreitung in spröden Werkstoffen im Biegeversuch", Thesis, University of Erlangen, FRG,1980.

[4]   R.J. Charles, "Dynamic fatigue of glass", J. Appl. Phys. 29 1657-1661(1958).

[5]   J.E. Ritter,Jr., "Engineering design and fatigue failure of brittle materials", in: Fracture Mechanics of Ceramics IV, Plenum Press, 1978,667-686.

[6]   T. Fett, D. Munz , "Determination of v-K_I-curves by a modified evaluation of lifetime measurements in static bending tests", Commun. of the Amer. Ceram. Soc. 68 C213-C215(1985).

[7]   T.E. Adams, D.J. Landini, C.A. Schumacher, R.C. Bradt, "Micro- and macrocrack growth in alumina refractories", Amer. Ceram. Soc. Bull. 60 730-35(1981).

[8]   K. Chen, Y. Ko, Amer. Ceram. Soc. Bull. 67 1228-1234(1988).

[9]   K.   Keller,   "Theoretische   und   experimentelle   Untersuchungen   zur Thermoermüdung keramischer Werkstoffe", Thesis, University of Karlsruhe, FRG, 1989.

[10] T. Fett, K. Keller, D. Munz, "Determination of crack growth parameters of alumina in 4-point bending tests", NAGRA Technical Report 85-51, Sept. 1985.

[11] T. Fett, D. Munz, "Subcritical extension in Ceramics", MRS-Conference, Tokyo, 1988.

[12] B. Gross, J.E. Srawley, "Stress intensity factors for three-point bend specimens by boundary collocation", NASA TN D-3092, 1965.

[13] W. Hermansson, "Determination of slow crack growth in isostatically pressed Al_2O_3, in: [14].

[14] The Swedish Corrosion Institute and its Reference Group: "Aluminium oxide as an encapsulation material for unreprocessed nuclear fuel waste - evaluation from the viewpoint of corrosion" Technical Report 80-15, KBS, Stockholm 1980.

[15] M. Mißbach, T. Fett, D. Munz, "Untersuchungen zum Versagen glasphasehaltigen Aluminiumoxids im Kriechbereich" Werkstoff-Kolloquium 5/6 April 1989, Stuttgart.
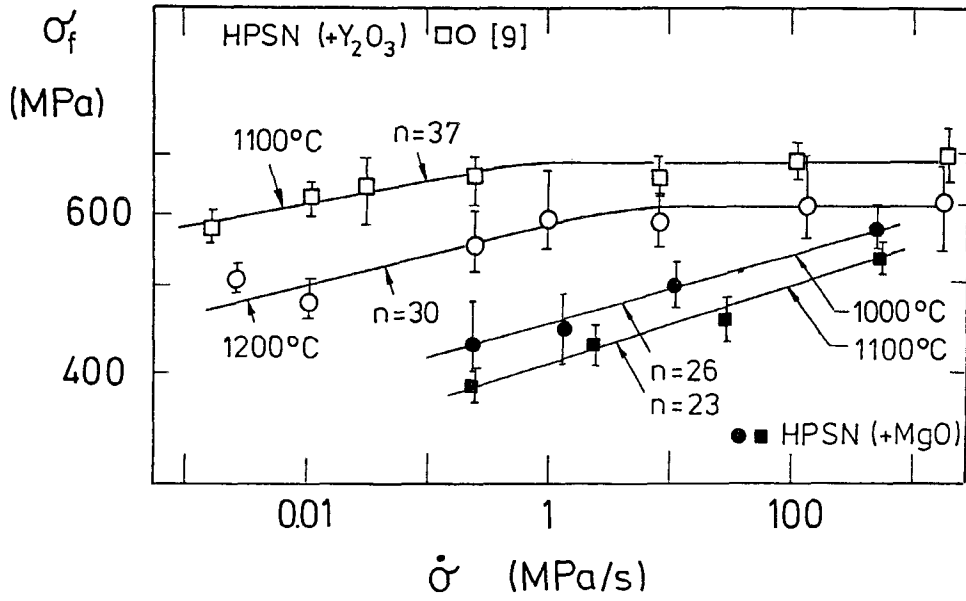
Fig.1

Dynamic bending strength of hot-pressed silicon nitride.
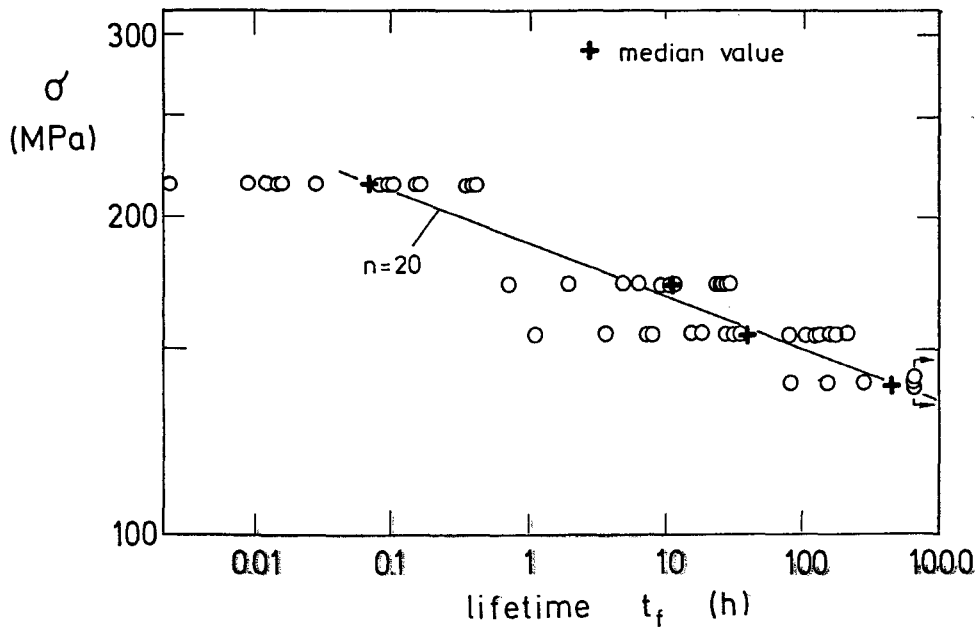
Fig.2 Lifetimes of Al_2O_3 in a high concentrated salt solution.
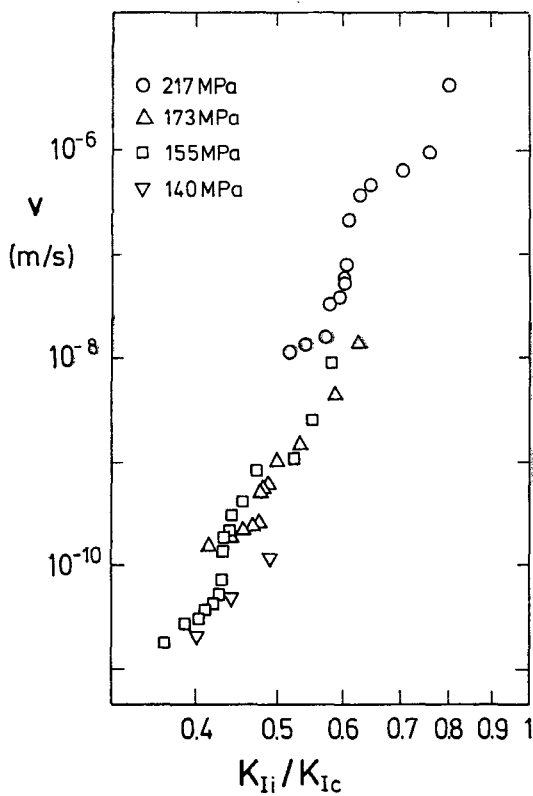
Fig.3
Crack growth rates for Al_2O_3 in concentrated salt solution.
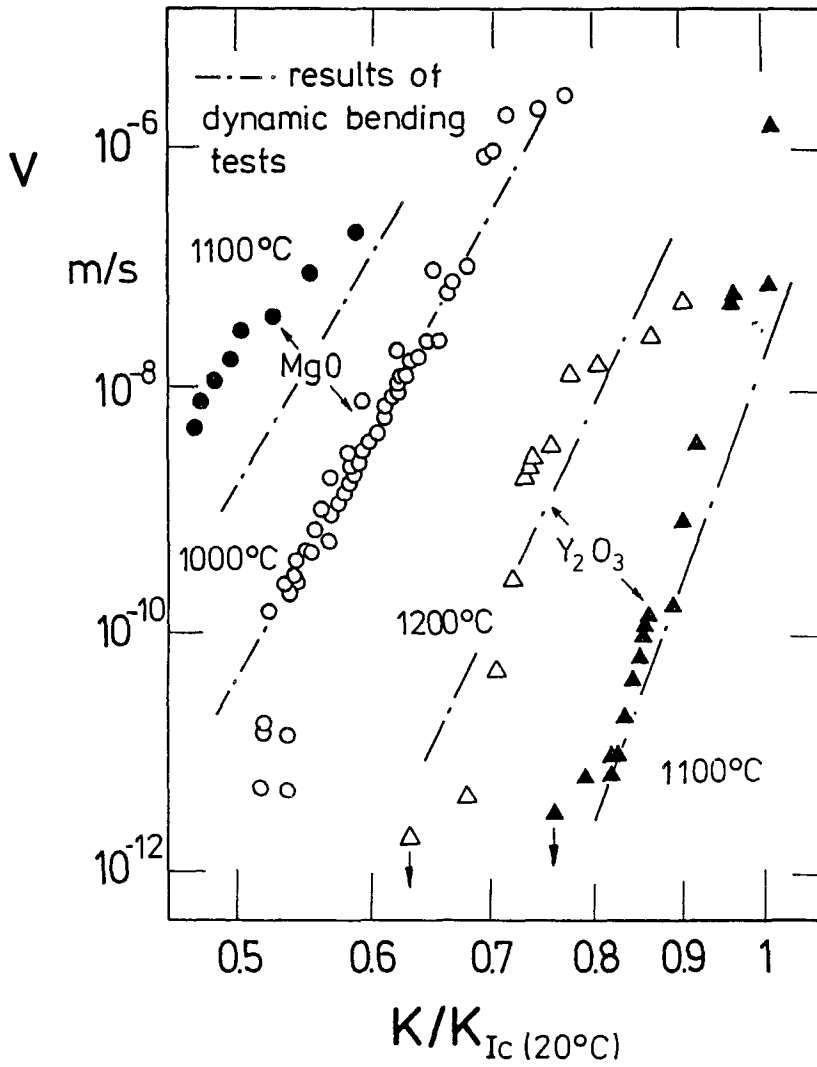
Fig.4

Crack growth rates for HPSN at high temperatures.
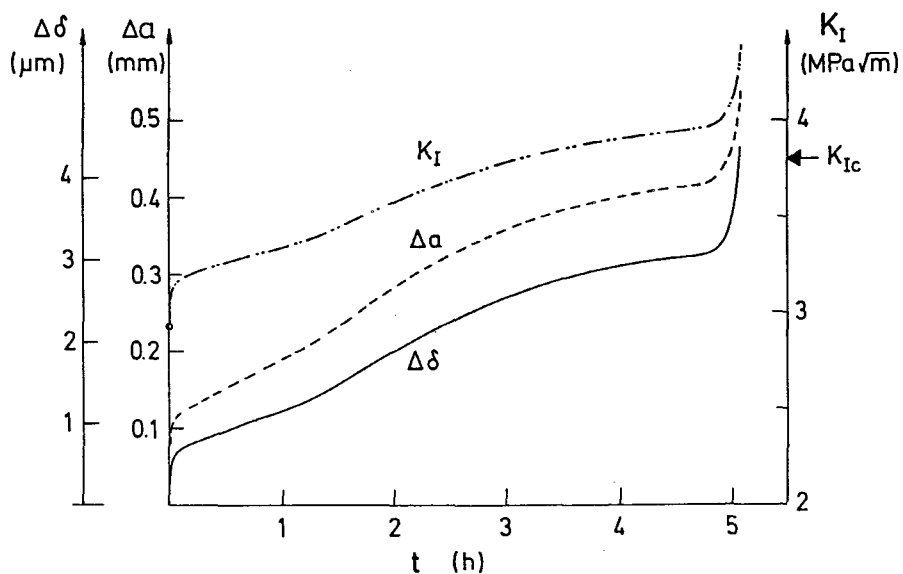
Fig.5

Displacements, crack length and the actual stress intensity factor K_I.
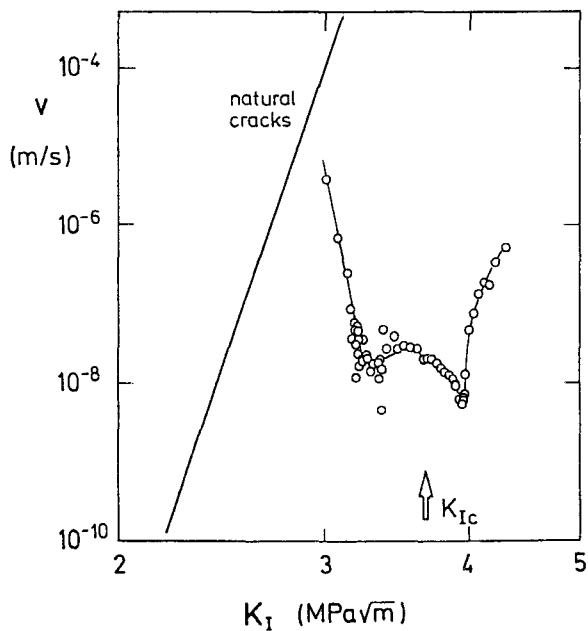
Fig.6

v-K_I curves for natural cracks compared with the
results of notched bending bars.
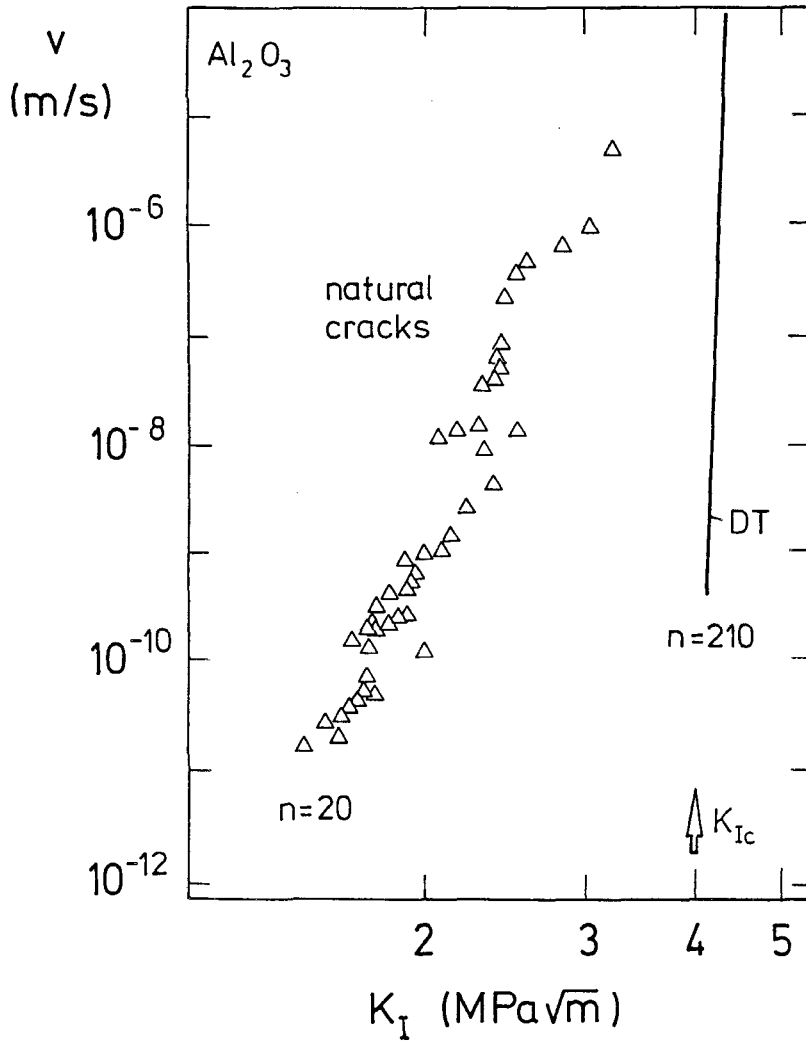
Fig.7

v-K_I curve for natural cracks compared with Double-Torsion results.
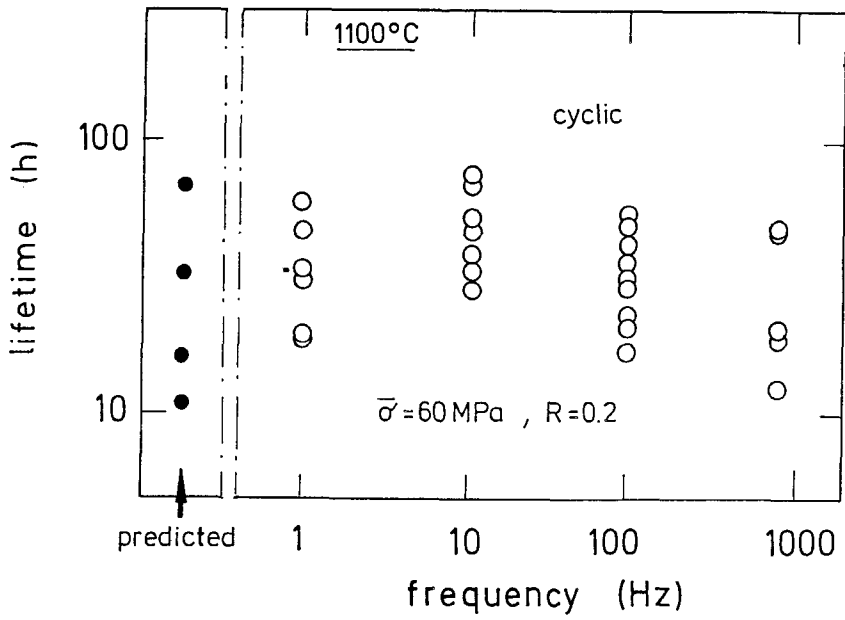
Fig.8

Lifetimes in cyclic bending tests obtained for Al_2O_3 containing 2.7% SiO_2.
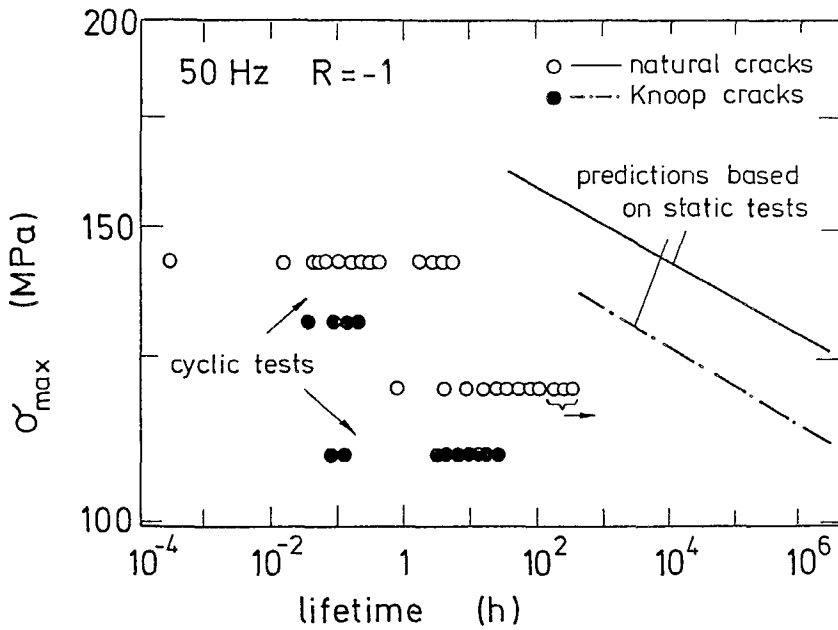
Fig.9

Predicted and measured lifetimes in cyclic bending tests for Al_2O_3 with natural cracks and Knoop-cracks.